PB-228 320

CONTINUOUS WATER POLLUTION SURVEILLANCE OPERATIONS, POTOMAC RIVER AT WASHINGTON, D. C. JULY 19, 1963-DECEMBER 31, 1964

Public Health Service
Washington, D. C.

June 1965

DISTRIBUTED BY:

NTIS

National Technical Information Service
U. S. DEPARTMENT OF COMMERCE
5285 Port Royal Road, Springfield Va. 22151

TD425.8
C6W3

PB 228 320

Ellet Lab
Library

CONTINUOUS WATER POLLUTION SURVEILLANCE OPERATIONS

Potomac River at Washington, D. C.

July 19, 1963 - December 31, 1964

Water Quality Section

Basic Data Branch

Division of Water Supply and Pollution Control

Public Health Service

Department of Health, Education, and Welfare

June 1965

1046

35

CONTINUOUS WATER POLLUTION SURVEILLANCE OPERATIONS

Potomac River at Washington, D. C.

July 19, 1963 - December 31, 1964

Summary

The Public Health Service has operated a continuous electronic water pollution monitor on the Potomac River at Washington, D. C. since July 19, 1963. The monitor provides a virtually continuous record of water temperature, specific conductance, pH, chloride and dissolved oxygen concentrations, and solar radiation intensity.

Water temperatures ranged from 33 to 87 degrees Fahrenheit and showed a significant amount of short-term variability during afternoons of bright, sunlit days. Specific conductance and chlorides varied from 120 to 490 µmhos and 3 to 55 mg/l respectively and were inversely proportional to the flows. Dissolved oxygen and, to a lesser extent, pH were most responsive to temperature and the action of photosynthesis, which in turn are normally dependent on the prolonged intensity of solar radiation. Dissolved oxygen varied from 2 to 15 mg/l and had minimum values below 4 mg/l on 21 days during the summer of 1964. There were evening increases in pH on week days during the winter months, presumably the result of industrial wastes, which were apparently overshadowed in warmer months by the effects of photosynthesis.

Spectral analyses of September 1963 and April 1964 dissolved oxygen and specific conductance data showed significant effects from the 12-hour semidiurnal and 14-day lunar fortnightly tides.

The PHS Potomac River electronic water pollution monitor is serviced by an experienced professional staff. Even so, data were missing because of all operational factors 16 per cent of the time.

Introduction

The U. S. Public Health Service has maintained the continuous operation of an electronic water pollution monitor on Memorial Bridge at Washington, D. C. since July 19, 1963. The monitor is located about 97 miles above the mouth and operated as a part of the Potomac River Water Pollution Surveillance System (see Figure 1). Water is pumped to the monitor from an elevation eleven feet above the stream bed. The depth of the intake varies from about four to eight feet. This report summarizes the operations and presents an initial interpretation of the data for the period July 19, 1963 through December 31, 1964.

Water temperature, conductivity (specific conductance at 25° C), concentration of chlorides, pH values, dissolved oxygen concentration and solar radiation intensity are recorded on a standard 10-inch strip chart. Daily maxima and minima are recorded manually and replotted to show general trends. Individual values are tabulated for periods selected for more intensive study which vary from one to 31 days. This involves reading levels of conductivity, dissolved oxygen, and water temperature which are plotted every six minutes, and values for the remaining parameters recorded at twelve minute intervals.

Electronic monitor data are summarized on Figures 2 and 3. Hydrologic and meteorological data shown on Figure 4 are from U. S. Weather Bureau records[1]. Tidal data, also shown on Figure 4, are from U. S. Coast and Geodetic Survey tide tables[2,3].

Geography and Hydrology

The Potomac River drainage basin includes 14,700 square miles of which about 80 per cent are above Washington, D. C. The river is approximately 400 miles long, flowing from the eastern slope of the Allegheny Mountains to Chesapeake Bay. Elevations within the basin range from sea level to nearly 5,000 feet in the Alleghenies. Annual precipitation averages about 40 inches near the coast. The average temperature throughout the basin is about 54° F with extremes of minus 30° and plus 112° F recorded.

Average flow (adjusted for diversions) of the Potomac River near Washington, D. C. for the 30-year period ending in 1960 was 11,100 cubic feet per second (cfs). Flows were much less during the study period and averaged only 9,300 cfs for the water year ending September 30, 1964. Rainfall in 1964 was about 29-1/2 inches.

The Potomac River is tidal up to Little Falls, Maryland, about 4-1/2 miles above the monitor. Tides are semidiurnal with an average range a little over three feet. Tidal influence is reflected by several of the parameters.

General Evaluation of Monitoring Data

Water Temperature. Water temperatures followed the annual cycle of air temperatures, and ranged from about 33° F in the winter to the upper 80's during the summer months. Although the actual water temperatures

probably dropped to 32° F in the winter, the recorded values were slightly higher because the intake line is heated to prevent freezing.

Diurnal variations averaged about 2° F. Short-term random variations, almost entirely in the afternoon, were superimposed upon the normal diurnal curve. Daily maxima usually occurred at or just before sunset, and minimum water temperatures occurred most often at about sunrise.

The persistence of random short-term afternoon or evening temperature variations led to an investigation of temperature over the length of the record. These variations occurred throughout the week indicating that waste discharges were not likely causes. Inspection of the solar radiation data showed a strong correlation between the two events. The variations were the greatest on very sunny days. Conversely, on days when the intensity of the sunlight was slight, short-term temperature variations were almost negligible.

Specific Conductance. Seasonal variations in specific conductance reflect patterns of stream flow. Levels of conductivity were highest during late summer and fall when the lowest flows were recorded. Temporary drops in conductivity coincided with heavy rains. The data for the last half of 1964 were about 10 per cent higher than that for the same period in 1963 due to the lower flows which occurred during 1964. Throughout the year, specific conductance ranged from about 100

micromhos in the winter and spring to as much as 450 micromhos during the fall.

Chlorides. Chloride concentrations were, with minor exceptions following autumn rains consistent with conductivity; high concentration coincident with low flow, and vice versa. Concentrations varied from less than 5 milligrams per liter (mg/l) during the winter to over 50 mg/l in late autumn of 1964.

Interrelationships of chloride concentration and conductivity for the period of record are shown on Figure 5. The relationship can be seen to be almost linear, with chloride concentrations in mg/l generally between 2 to 10 per cent of the conductivity in micromhos. An envelope drawn from data reported by the U. S. Geological Survey[4] is also shown on Figure 5. The Public Health Service points were arbitrarily selected from the 1-1/2 years of continuous monitor data. The agreement between PHS and GS data is as good as can be expected in view of the difference of sampling dates and locations. The discontinuity in slope of the GS data is almost certainly due to the limited sample size.

pH. pH varied between 6.5 and 10.0 during the period of record. Short-term variations followed and were consistent with dissolved oxygen levels during the summer when the water was warm and there was a great deal of photosynthetic activity.

In the winter of 1963-64 and beginning again in December 1964, daily temporary increases in pH occurred during the evening hours (see Figure 6). These variations appeared as small peaks of as much as 0.4 pH units and generally lasted no more than three hours. These peaks occurred on weekdays only, suggesting that municipal or industrial discharges were responsible. This pH variability was only recognizable during the very cold months of mid-winter and are presumably overshadowed by large pH variations associated with photosynthesis during the rest of the year.

Dissolved Oxygen. Concentrations of dissolved oxygen followed the annual cycle of low concentrations in the summer when water temperature was high, and high concentrations in the winter. This minimum dissolved oxygen concentration of 2.0 mg/l was observed on August 4, 1964. Figure 3 shows this event followed by one week a high concentration of 10.0 mg/l, and corresponding saturation value of 127%, which suggest a plankton bloom which subsided during the interval. During the summer of 1963, the minimum dissolved oxygen concentration was 4.2 mg/l, while in 1964, between June 16 and September 4, minimum values less than 4.0 mg/l occurred on 21 of the 73 days during which the monitor was operating satisfactorily. Maximum concentrations of about 15 mg/l in the winter were in accord with the greater solubility of oxygen in the colder water. Diurnal variations were greatest in the summer, coinciding with highest levels of photosynthesis.

Solar Radiation. Solar radiation intensity was detected by an Eppley pyrheliometer mounted on the piling on the downstream side of the bridge. Figure 7 compares the monitoring station data with that obtained by the U. S. Weather Bureau data taken at Sterling, Virginia, approximately 20 miles away. On clear days, the levels at the two stations are generally within about 20 per cent. Larger variations were, as expected, found on cloudy days. Both installations show the annual variation in sunlight, and the Weather Bureau data have consequently been shown on Figure 4.

A detailed comparison of short-term variations in solar radiation intensity and in dissolved oxygen was made for the days during which partly cloudy weather was indicated by the monitor. Figures 8A and 8B show six typical days when solar radiation was variable. The variations in dissolved oxygen are shown to have been the result of photosynthesis depending on total radiation throughout the day and of tidal stage. The brief periods of either extremely high or low intensities were not reflected in dissolved oxygen at the depth sampled.

Power Spectrum Analyses

In recent years, the analysis of sequential data such as those generated by the automatic water quality monitor has been greatly facilitated by the use of power spectrum analysis. A simplified

description of the mathematics has been published by Wastler[5]; this is summarized in Appendix A.

Wastler also showed the application of spectral analysis to estuarial data, particularly from the Potomac River. Computation of individual power spectra indicates the frequencies at which significant portions of the variance are found as well as an estimate of the amounts of variance which occur at these frequencies. It is accordingly possible to estimate the relative dependence of dissolved oxygen concentrations and conductivity upon sunlight, tides, and other factors which occur at regular intervals. Such estimates are useful in checking the validity of oxygen balance computations. Data from two 31-day periods, August 27-September 26, 1963 and April 1-May 1, 1964 were studied. The results of these analyses are listed in Table 1.

Table 1

RESULTS OF SPECTRAL ANALYSIS

	Dissolved Oxygen		Specific Conductance	
	8/27 to 9/26/63	4/1 to 5/1/64	8/27 to 9/26/63	4/1 to 5/1/64
Mean	6.07 mg/l	10.67 mg/l	371.4 µmhos	181.4 µmhos
Standard deviation	0.57 mg/l	1.07 mg/l	42.5 µmhos	24.8 µmhos
Estimated portion of total variance due to:				
Secular trends plus random variations at lag 0	5%	60%	60%	65%
Water depth:				
Lunar fortnightly tide (14-day period)	53%	0.0%	0.0%	0.0%
Lunar semidiurnal tide	4.3%	0.0%	0.3%	0.3%
Sunlight (24-hr. period)	5.2%	1.3%	0.0%	0.0%

Differences in mean concentrations during the two periods reflect annual cycles of hydrographic and meteorological factors. The analyses of August 27-September 26, 1963 used sampling intervals ranging from 6 minutes to 6 hours, while those of the analyses of April 1-May 1, 1964 were based on intervals from 1/2 to 2 hours. Longer intervals are used to identify longer period variations. Additional variations at periods of less than 12 hours were also identified. These constitute much less than 1% of the total variance and are probably due to seiches in which water levels fluctuate at the resonant period of the particular water body. The segments of the estuary which are involved with these seiches have not been identified. The percentages of total variance at lag 0 were generally consistent with secular trends shown on Figure 2.

A more comprehensive evaluation of the spectral analyses is presented in a separate publication[6].

Monitoring Equipment Operations

A record of continuous monitor operations is shown on Figure 9. Breaks in this record occurred during 16 per cent of the time and were due to a variety of causes. On March 4 the pump supplying the water to the monitor failed. Solar radiation data are not affected by such a failure. A replacement pump was put into operation on March 17. All parameters were again monitored except for dissolved oxygen which became operational again on March 26 upon installation of a new D.O. probe.

On July 4 the solar radiation sensor was broken and was subsequently replaced in mid-October. Between August 6 and August 13, 1964, no data were obtained because of mechanical malfunction of the printing wheel; this was remedied by cleaning and oiling. Additional causes of breaks in the record include power failure, cleaning and replacing probes, calibration checks, replacement of charts, and preventive maintenance on the monitor. The overall performance of this equipment represents the optimum which may be expected from an installation which receives weekly servicing from an experienced professional staff.

REFERENCES

1. Weather Bureau Local Climatological Data, Department of Commerce, National Airport, Washington, D. C., monthly from July 1963 to December 1964.

2. Tide Tables, High and Low Water Predictions, East Coast North and South America including Greenland, 1963. Department of Commerce, Coast and Geodetic Survey.

3. Tide Tables, High and Low Water Predictions, East Coast North and South America including Greenland, 1964. Department of Commerce, Coast and Geodetic Survey.

4. Durfor, C. N. Water Quality and Hydrology in the Fort Belvoir Area, Virginia, 1954-55. U. S. Geological Survey Water-Supply Paper 1586-A (1961).

5. Wastler, T. A. Applications of Spectral Analysis to Stream and Estuary Field Surveys. I. Individual Power Spectra. Department of Health, Education, and Welfare, Public Health Service, Robert A. Taft Sanitary Engineering Center (1963).

6. Gunnerson, C. G. Optimum Sampling Interval for Water Quality Monitoring in Tidal Estuaries. Paper presented at ASCE National Symposium on Sanitary Engineering Research, Development, and Design, July 1965.

Appendix A

THE ARITHMETIC OF POWER SPECTRUM ANALYSIS*

Power spectrum analysis is one method for time-series analysis. The term is usually abbreviated to spectral analysis. Spectral analysis provides measures of the variance of a record. Variance is expressed as the mean square or power of the units being measured; hence, "power spectrum analysis."

A time series is a record of repeated observations made at a particular location. Each observation is a momentary summation of the effects of everything that is happening to the particular parameter. These effects may be caused by cyclic or random phenomena. A trend throughout a given record length may be real or apparent; for example, a short segment of a sine wave will appear as a trend.

Power spectrum analysis identifies the frequencies at which different factors cause the record to vary. The analysis also provides an estimate of the variance which derives from each of these factors.

---

*This appendix is based upon, "Application of Spectral Analysis to Stream and Estuary Field Surveys. I. Individual Power Spectra," by T. A. Wastler, USPHS Publication No. 999-WP-7, 1963.

Figure A1 shows some simple spectra (more precisely, estimates of spectral density) from several types of curves. Where the original curve is made up of more than one factor, as in cases V and VI, the power spectrum clearly reveals the nature of the components.

Four steps in the computation of individual pwer spectra are as follows:

I. The mean and the square of the mean of the record are determined.

II. The autocorrelation function of the record is formed. This is the basic operation in spectral analysis, and it is described in detail below.

III. The Fourier cosine transform for each autocorrelation is computed. This defines the difference between spectral analysis and standard Fourier analysis since in the latter, the Fourier transform is applied to the raw record rather than autocorrelation function. In spectral analysis, the Fourier transform serves to smooth out some of the fluctuations present in the autocorrelation function.

IV. A second weighting operation provides the estimate of spectral density.

The Autocorrelation Function

Wastler's description is essentially as follows. The autocorrelation function is obtained by first multiplying each number in the record by another number in the record. From the mean of the sum of these products is subtracted the square of the arithmetic mean of the entire series. In determining the autocorrelation at lag 0, the record is multiplied by itself so that the result is the variance as defined in statistics. The autocorrelations ag lag 0, lag 1, lag 2, and lag 3 are computed as shown in Table A1.

Table A1

TYPICAL COMPUTATION OF AUTOCORRELATION FUNCTION

$C_0 \equiv$ Autocorrelation at lag 0	$C_1 \equiv$ Autocorrelation at lag 1	$C_2 \equiv$ Autocorrelation at lag 2
1.30 x 1.30 = 1.69	1.30 x 2.57 = 3.34	1.30 x 3.79 = 4.93
2.57 x 2.57 = 6.60	2.57 x 3.79 = 9.74	2.57 x 1.49 = 3.83
3.79 x 3.79 = 14.36	3.79 x 1.49 = 5.65	3.79 x 2.30 = 8.72
1.49 x 1.49 = 2.22	1.49 x 2.30 = 3.43	1.49 x 4.73 = 7.05
2.30 x 2.30 = 5.29	2.30 x 4.73 = 10.88	2.30 x . .
4.73 x 4.73 = 22.37	4.73 . .	4.73 x . .
. .	. . .	. . .
. .	. . .	. . .
. .	. . .	. . .
. .	. . .	. . .
3.10 x 3.10 = 9.61	3.10 x 1.46 = 4.53	3.10 x 3.16 = 9.80
1.46 x 1.46 = 2.13	1.46 x 3.16 = 4.61	1.46 x 3.30 = 4.82
3.16 x 3.16 = 9.99	3.16 x 3.30 = 10.43	3.16 x 1.41 = 4.46
3.30 x 3.30 = 10.89	3.30 x 1.41 = 4.65	3.30 x 2.35 = 7.76
1.41 x 1.41 = 1.99	1.41 x 2.35 = 3.31	1.41
2.35 x 2.35 = 5.82	2.35	2.35
Sum = 1046.9	Sum = 804.67	Sum = 764.62
$\frac{1046.9}{145} = 7.22$	$\frac{804.67}{144} = 5.588$	$\frac{764.62}{143} = 5.347$
-5.90	-5.90	-5.90
$C_0 = 1.32$	$C_1 = -0.312$	$C_2 = -0.553$

NOTE: Number of observations = 145; Mean of observed values = 5.90.

The entire operation may be expressed mathematically as

$$C_r = \frac{1}{n-r} \sum_{1}^{n-r} x_t x_{t+r} - \left[\frac{1}{n} \sum_{1}^{n} x_t\right]^2,$$

where

C_r = autocorrelation at lag r,
x_t = record value at t,
t = 0, 1, 2 ... n = sequential index of values,
r = 0, 1, 2 ... m = lag number,
m = total number of lags.

In the simple case of a pure sine wave, the computation is physically analogous to looking at white picket fence through one of a series of vertical gratings. Both the fence and the gratings are constructed so that the bar width always equals the slot width. The pickets are a square-wave approximation of the sine wave. The resolution or detail with which the fence may be seen is a function of the spacing between grates. Similarly, the resolution of the sine wave is a function of the number of lags used for computing the autocorrelation function.

If the spacing of the grates is too large, some of the pickets will not be seen. The total amount of light seen by the viewer will be less than the amount reflected by the fence. When the grating with the optimum spacing is selected, the fence can be described precisely. This also happens when the optimum number of lags is applied to the sine wave record.

As the grate spacing continues to be decreased, all of the pickets can still be seen, but some of the light is again lost to the viewer. Soon, only half the reflected light is available and eventually, the visual resolution of the fence is destroyed entirely because the grating

dimensions approach those of light waves. Here, interference and diffraction patterns are set up. Something comparable, though not strictly analogous, happens when the autocorrelation is computed to too many lags for the particular record length. The computation becomes unstable.

Figure A2 illustrates the autocorrelation functions of two pure sine waves and of their sum. Although the particular example is more simple than those found in nature, it shows how the number of lags (in this case, eight) relates to the description of the record by means of an autocorrelation function.

It can be seen intuitively that any variance due to a secular trend in the record will be measured at lag 0. This is because a secular variation has an infinite period (zero frequency). This value will, of course, be added to that due to harmonic motion.

Fourier Transform and Smoothed Spectrum

The Fourier cosine transform is calculated as follows:

$$V_r = \frac{k}{m}\left[C_0 + C_m \cos r\pi + 2\sum_{q=1}^{m-1} C_q \cos \frac{q r \pi}{m}\right],$$

where

V_r = Fourier cosine transform of the autocorrelation at lag r,

q = lag number, having values between 1 and m-1

k = a constant, k = 1 for r = 1, 2 ... m-1,
k = 1/2 for r = 0,
r = m,

and the other letters have the definitions previously given.

The smoothed estimate of spectral density is obtained from a final weighting function, expressed mathematically as:

$$U_0 = 0.54\, V_0 + 0.46\, V_1$$

$$U_r = 0.23\, V_{r-1} + 0.54\, V_r + 0.23\, V_{r+1}$$

for r = 1, 2, 3 ..... m-1

$$U_m = 0.46\, V_{m-1} + 0.54\, V_m$$

where U_0, U_r, U_m are the power spectrum estimates corresponding to the respective lags, and the remaining symbols have the meanings previously assigned.

Sample calculations of the smoothed spectrum are presented by Wastler.

Aliasing

The designs of both the sampling interval and the subsequent statistical or spectral analysis require consideration of aliasing. Aliasing is defined graphically on Figure A3 and results from high-frequency events which add variance to the record but which are not "seen" by the particular sampling interval.

Figure A3 illustrates how the variance from this type of event is folded into the record and reappears at a lower frequency. Where the period of the high-frequency event is known, the period of the aliased record can readily be determined analytically.

Inspection of Figure A3 reveals that any cyclic event which occurs at a period less than twice the sampling interval will result in aliasing. Where the period equals twice the sampling interval, the event will never be seen.* Only when the period exceeds twice the sampling interval can the event be measured. It is obvious that as the period of the cyclic event approaches a value of twice the sampling interval, the record length necessary to describe the event increases. The corresponding frequency, f_n, which limits the events, seen by a particular sampling frequency, f_s, is known as the Nyquist frequency, $f_n = 1/2\ f_s$.

General

The interrelationships between sampling interval, record length, number of lags, degrees of freedom, and confidence limits are discussed briefly by Wastler (14). Definitive treatments are presented in several of the works listed in the bibliography.

The bibliography also includes works which describe the calculation and interpretation of cross-spectra. These are basically a comparison of pairs of individual power spectra which produces the equivalent of correlation coefficients between time series measuring different events

---

Note. The same is true for any event whose period (P) is related to the sampling interval (I) by $P = 2I/n$ where n is a positive integer. In the design of sampling programs, those cases where $n > 1$ are not normally considered.

(e.g., tidal stage and salinity). In addition to providing a measure of the correlation or coherence between the two events, the phase relationship is established and other criteria are determined.

A SELECTED BIBLIOGRAPHY ON SPECTRAL ANALYSIS AND RELATED SUBJECTS

(1) Barber, N. F. Experimental Correlograms and Fourier Transforms. Pergamon Press, 1961.

This is an excellent introduction, most useful to the engineer or physical scientist, which clearly shows the physical significance of Fourier transforms, correlograms, and power spectra. The underlying theory and a wide variety of mechanical, optical, and electrical analogs are reviewed.

(2) Barber, N. F. and Tucker, M. J. Wind Waves. In The Sea, Vol. I. M. N. Hill, Editor, Interscience, 1962, pp. 664-699.

Presents example of need for and results from spectral analysis.

(3) Blackman, R. B. and Tukey, J. W. The Measurement of Power Spectra. Dover, 1958.

This is the standard reference for the theory and application of spectral analysis.

(4) Cartwright, D. E. Analysis and Statistics. In The Sea, Vol. I. M. N. Hill, Ed., Interscience, 1962, pp. 567-589.

Summarizes statistical formulation of sea waves and introduces concepts of spectral analysis.

(5) Dixon, W. J., Editor. BMD - Biomedical Computer Programs. Health Sciences Computing Facility, Department of Preventive Medicine and Public Health School of Medicine, University of California, Los Angeles, January 1, 1964.

Includes digital computer programs for individual power spectra, cross spectra, and other time-series analyses.

(6) Dronkers, J. J. Tidal Computations. Interscience 1964.

A basic and complete treatment of tidal hydrodynamics, harmonic analysis, and computational methods.

(7) Holloway, J. L., Jr. Smoothing and Filtering of Time Series and Space Fields. Advances in Geophysics, Vol. 4, Academic Press, 1958, pp. 351-389.

Reviews and presents basis for selection from a variety of methods for smoothing and filtering serial data.

(8) Munk, W. H., Snodgrass, F. E., and Tucker, M. J. Spectra of Low-Frequency Ocean Waves. Bull. Scripps Inst. Oceanog., Univ. of Calif., Vol. 7, No. 4, 1959, pp. 283-362.

Includes what the senior author identifies as a cookbook of numerical recipes.

(9) Panofsky, H. A. and Brier, G. W. Some Applications of Statistics to Meteorology, Pennsylvania State University Press, 1958.

Chapter VI, Time Series, is an excellent introduction to the subject.

(10) Rosenblatt, M., Editor. Time Series Analyses. Proceedings of the symposium held at Brown University, June 11-14, 1962, Wiley, 1963.

Includes papers on a broad range of topics, including statistical theory, spectral analysis, and applications to geophysical, engineering, economic and biological problems.

(11) Snodgrass, F. E., Munk, W. H., and Miller, G. R. Long-Period Waves over California's Continental Borderland. I. Background Spectra. Jour. Marine Res. Vol. 20, 1962, pp. 3-30.

Presents an example of results derived uniquely from spectral analysis of ocean waves.

(12) Southworth, R. W. Autocorrelation and spectral analysis. In Mathematical Methods for Digital Computers, by A. Ralston and H. S. Wilf, Editors. Wiley, 1960, pp. 213-220.

Presents digital computer program for determining autocorrelation function.

(13) Stommel, H. Varieties of Oceanographic Experience. Science, Vol. 139, 1963, pp. 572-576.

Presents magnitudes and interrelationships of time and space characteristics for both sea level and ocean currents.

(14) Wastler, T. A. Application of Spectral Analysis to Stream and Estuary Field Surveys. I. Individual Power Spectra. U. S. Public Health Service Pub. No. 999-WP-7, 1963.

A primer of mathematical basis for and application of spectral analysis.

(15) Wastler, T. A. Application of Spectral Analysis to Stream and Estuary Field Surveys. II. Cross Spectra (in preparation).

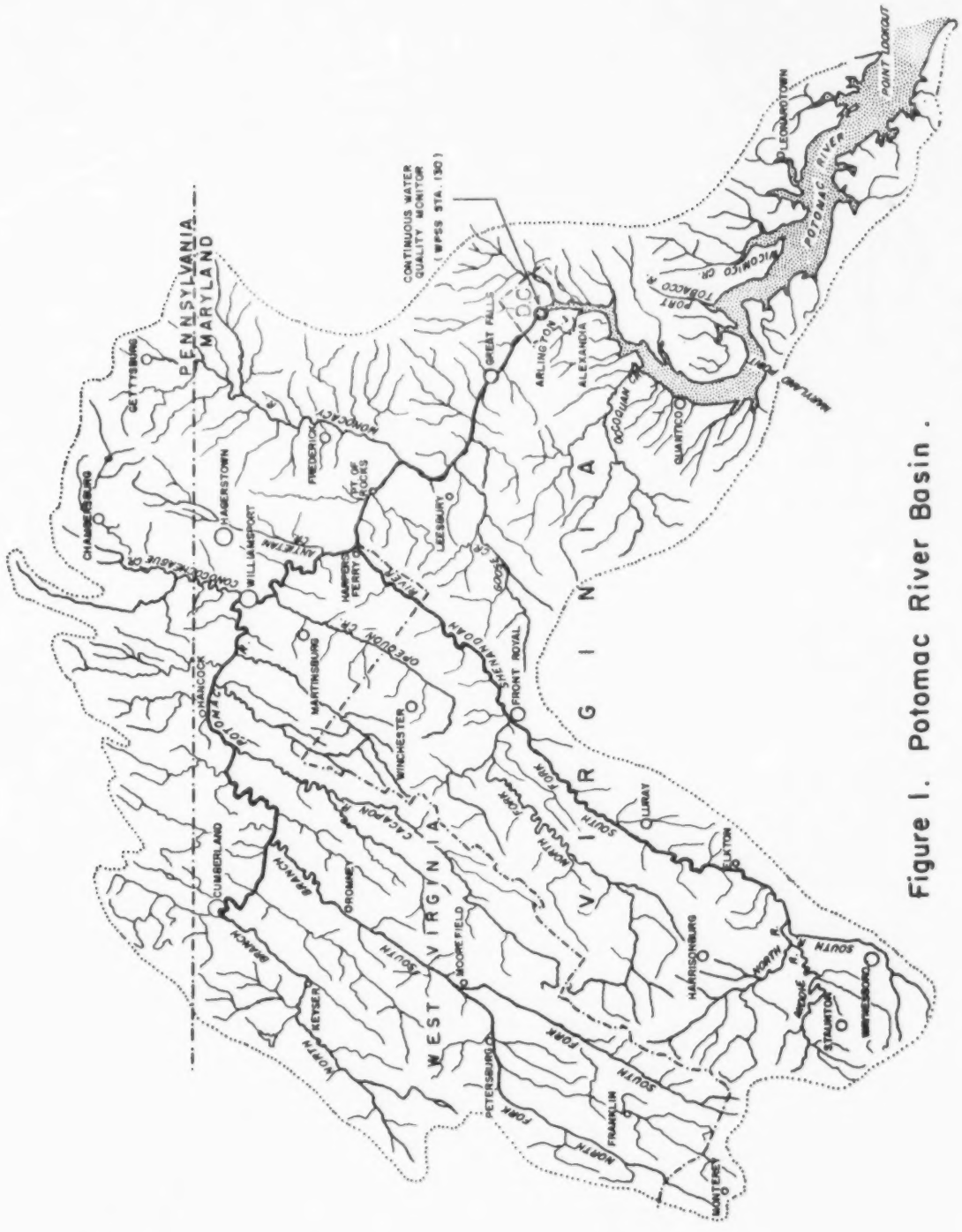

Figure 1. Potomac River Basin.

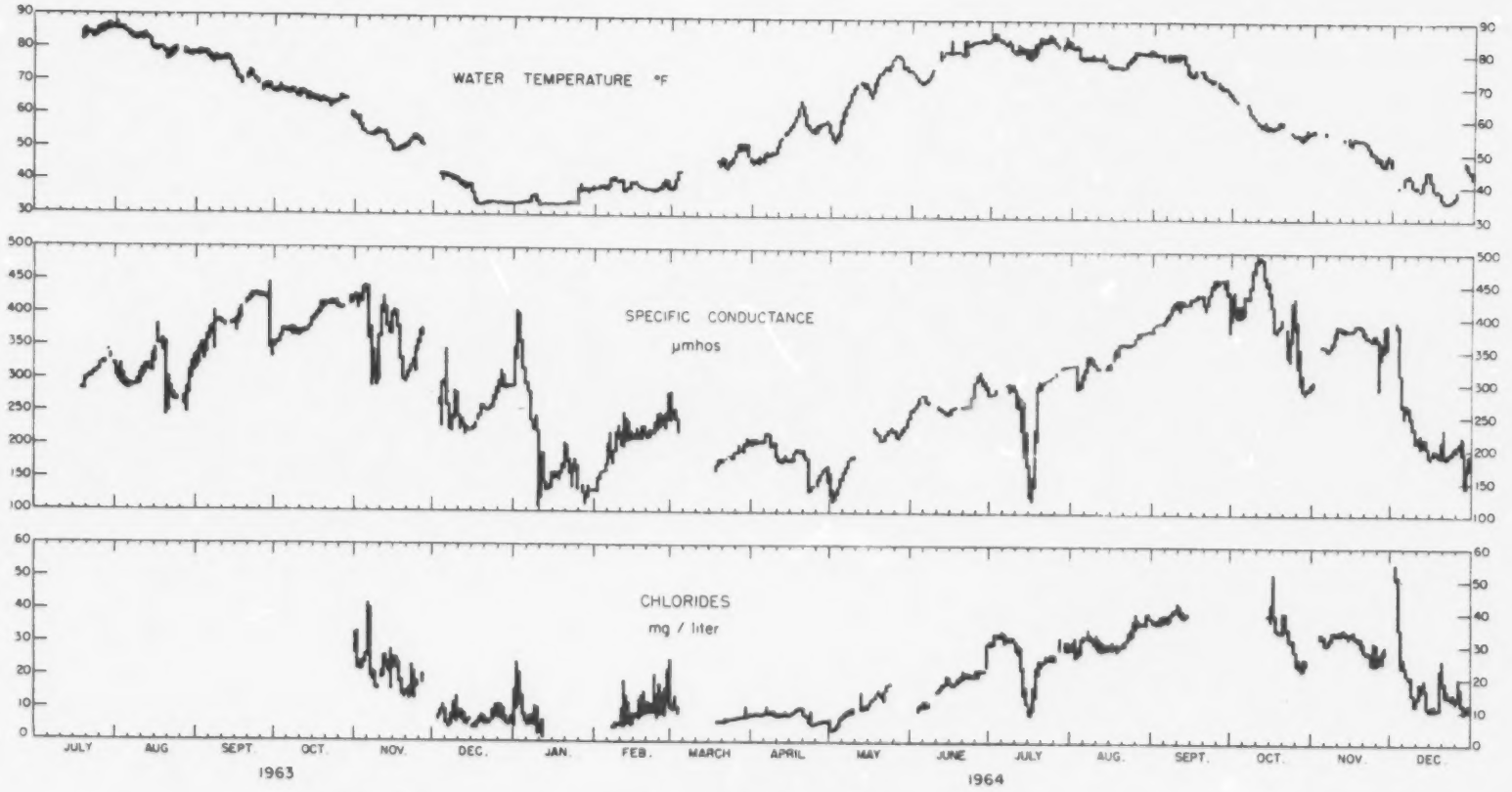

Figure 2. Summary of continuous monitoring data – Potomac River at Washington – daily ranges of temperature, specific conductance, and chlorides – July 1963 through December 1964.

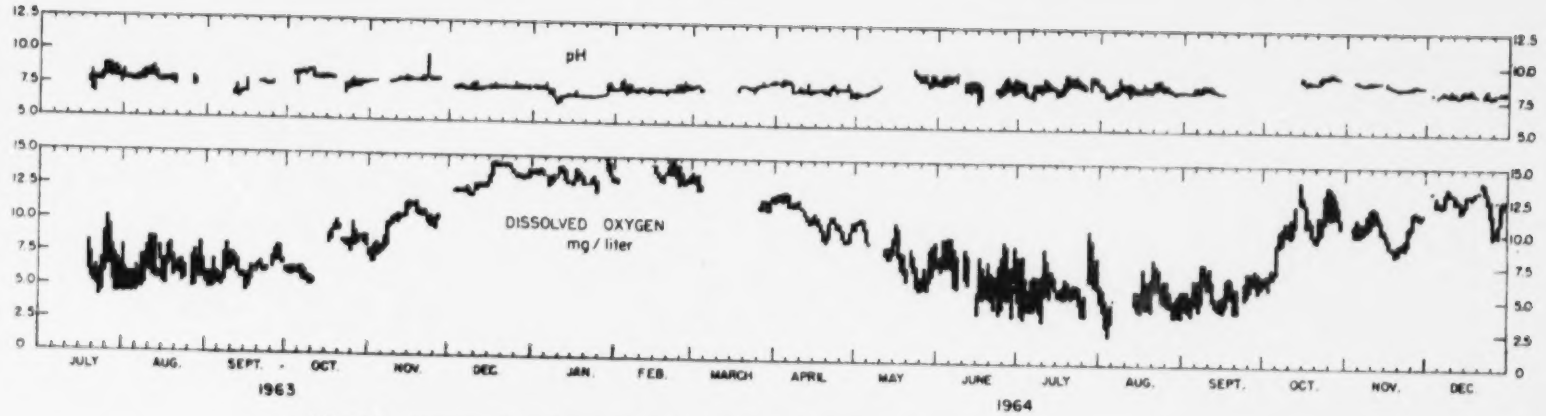

Figure 3. Summary of continuous monitoring data - Potomac River at Washington - daily ranges of pH and dissolved oxygen - July 1963 through December 1964.

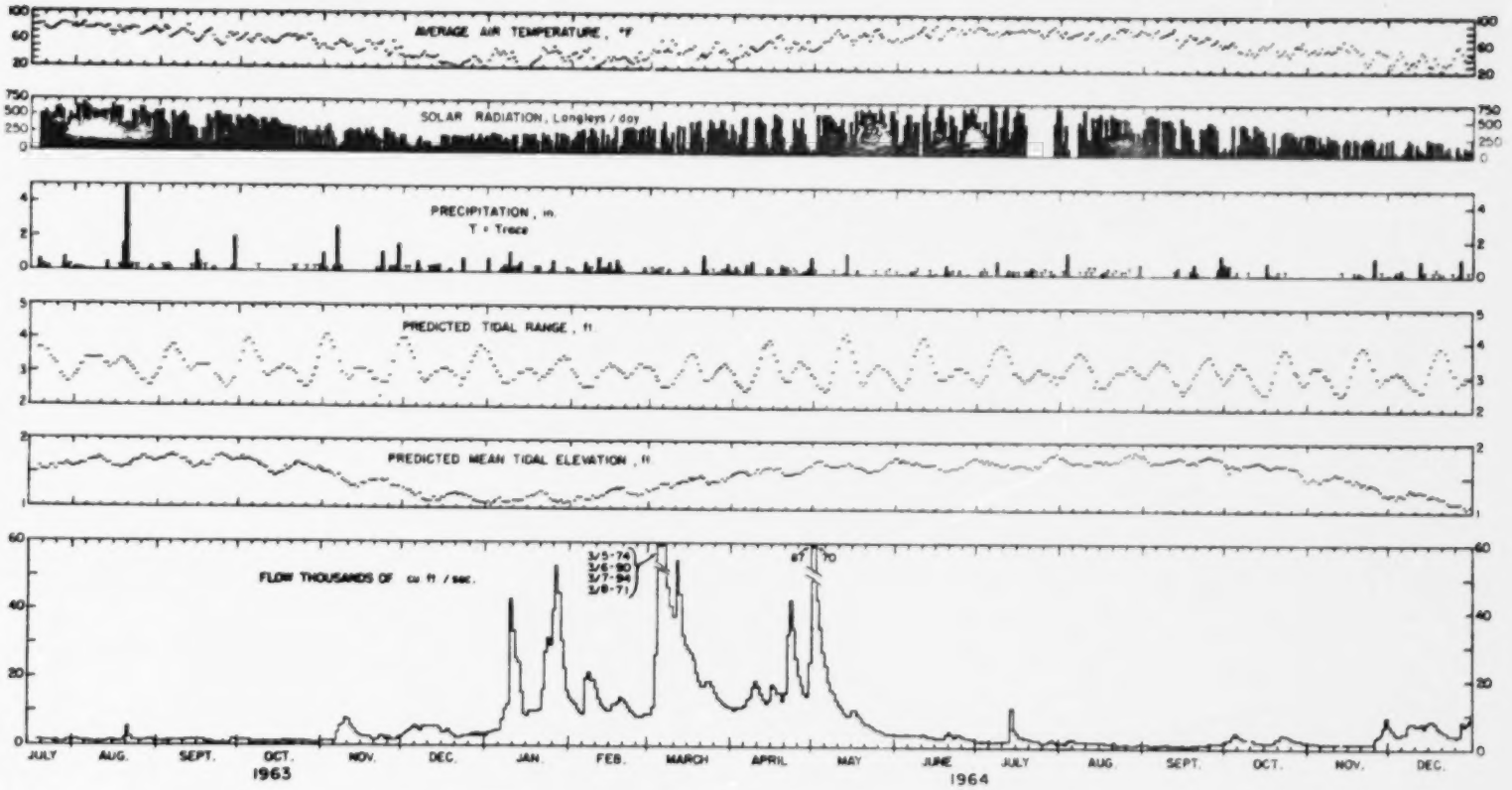

Figure 4. Meteorological and hydrographic data – Potomac River at Washington July 1963 through December 1964.

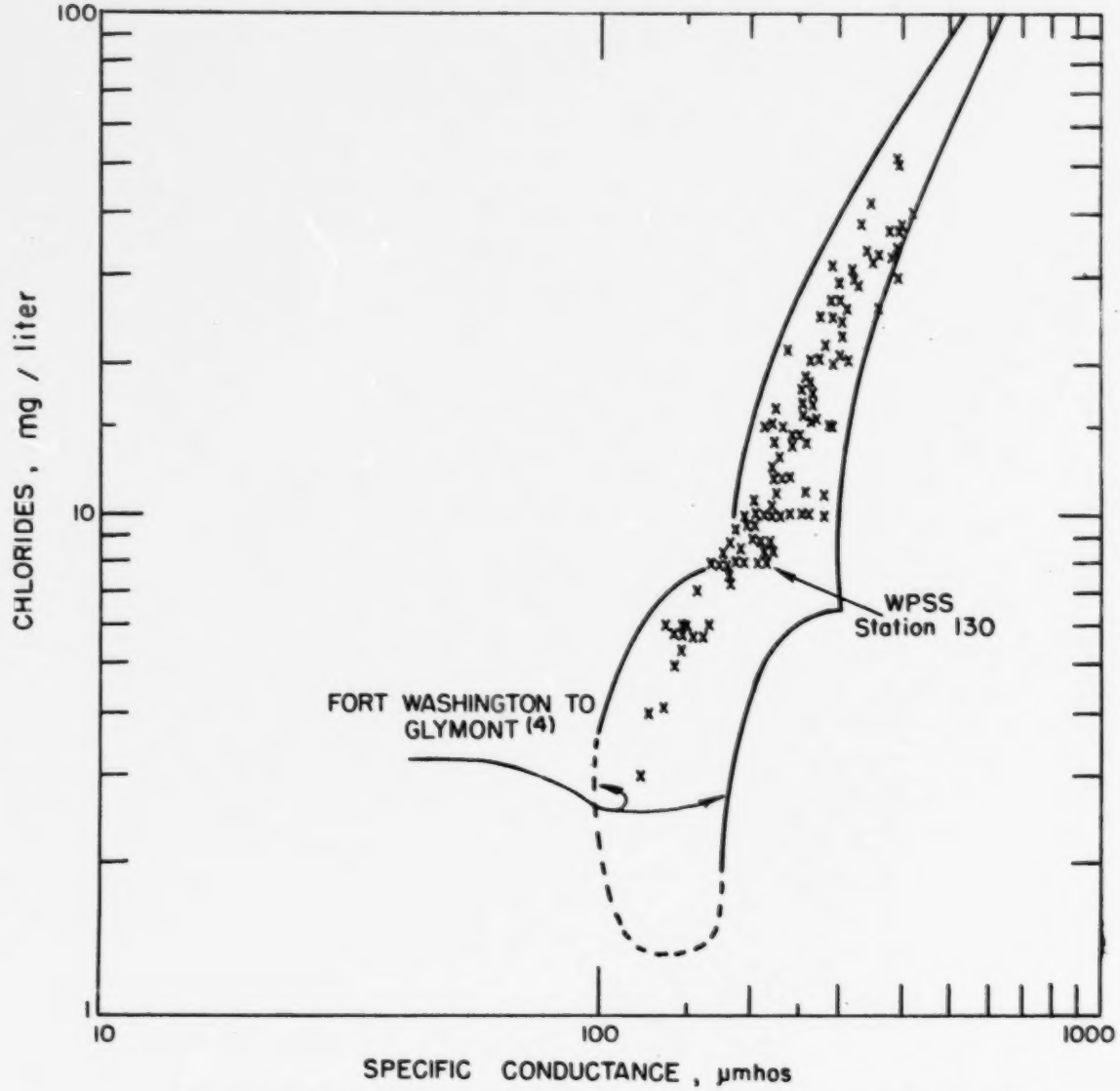

Figure 5. Interrelationships of chlorides and specific conductance in Potomac River.

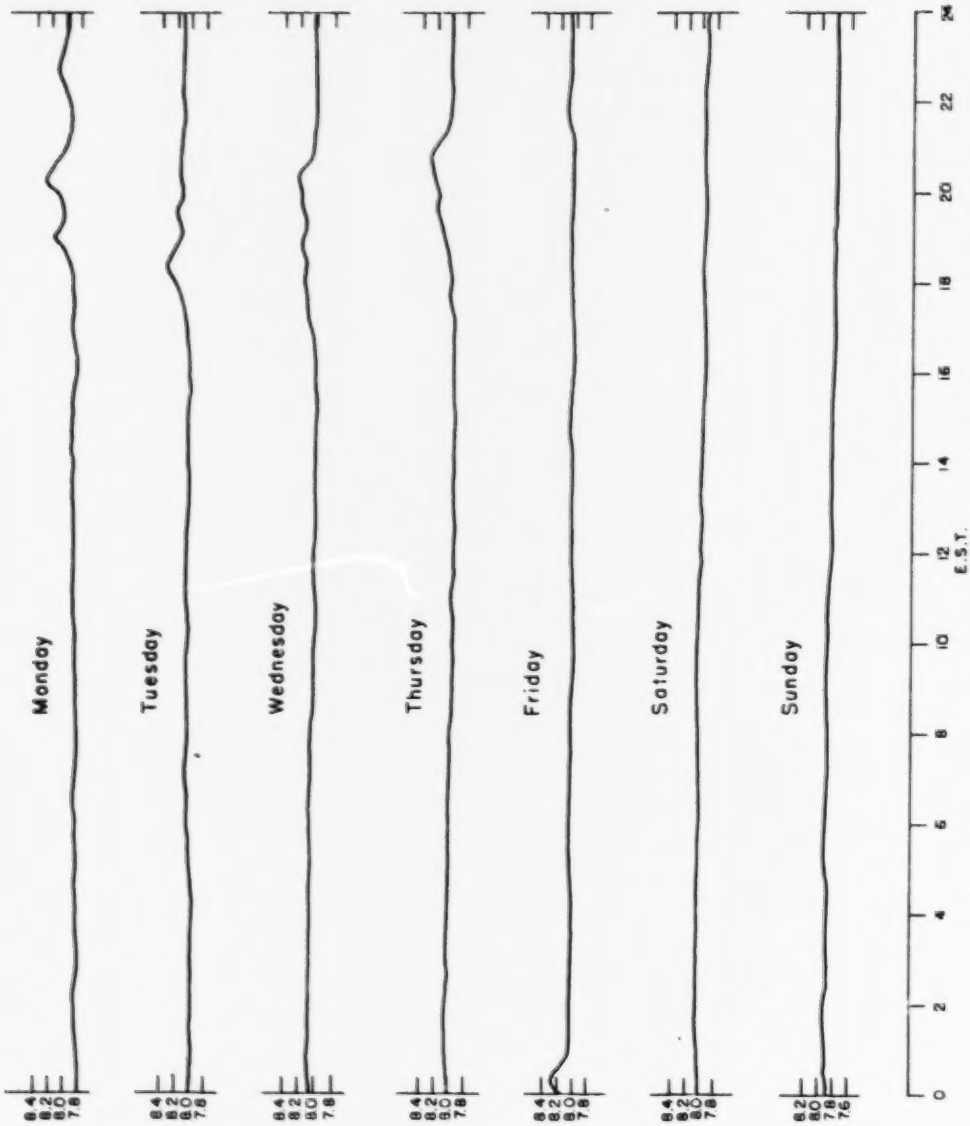

Figure 6. Short-term variations in pH
December 14 – 20, 1964

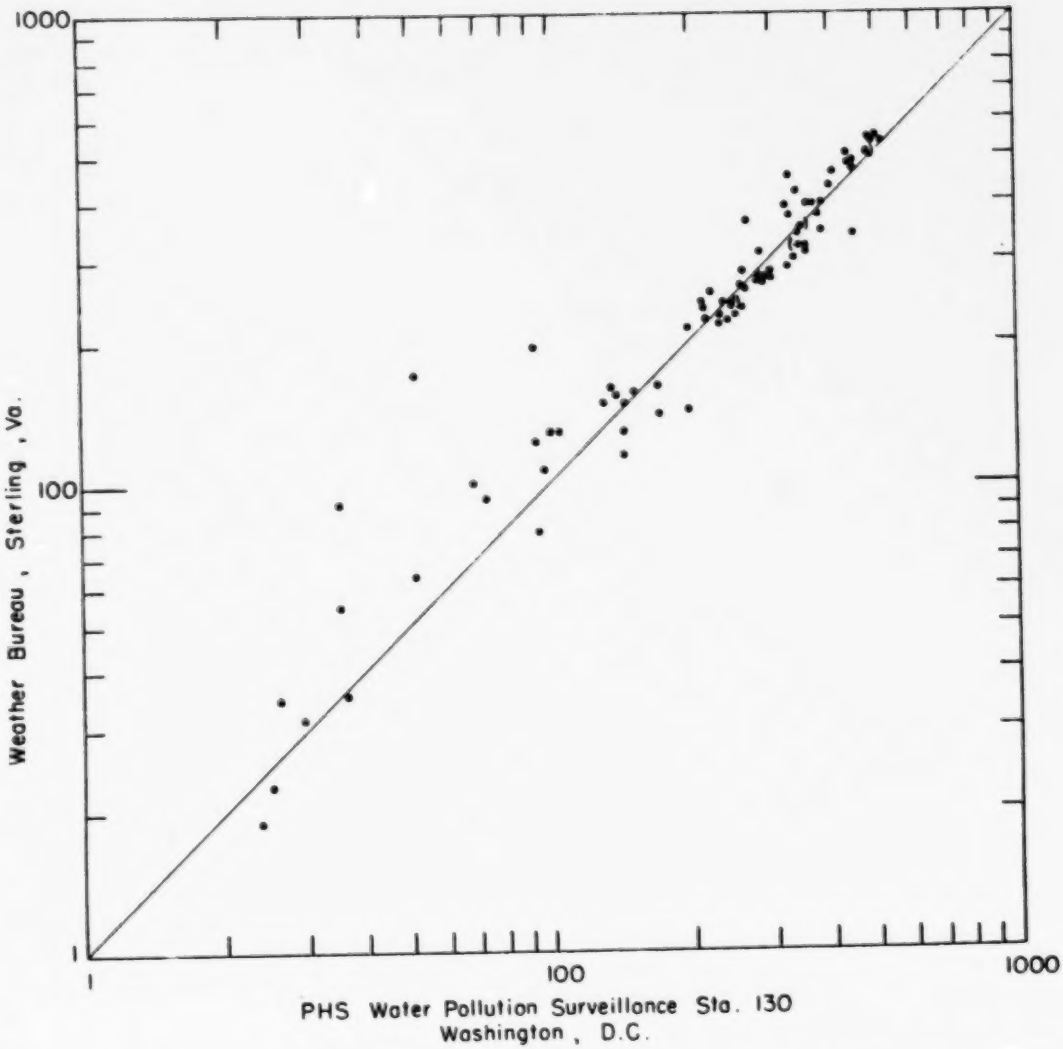

Figure 7. Comparison of daily solar radiation in langleys per day at Sterling , Va. (USWB) and Washington (PHS).

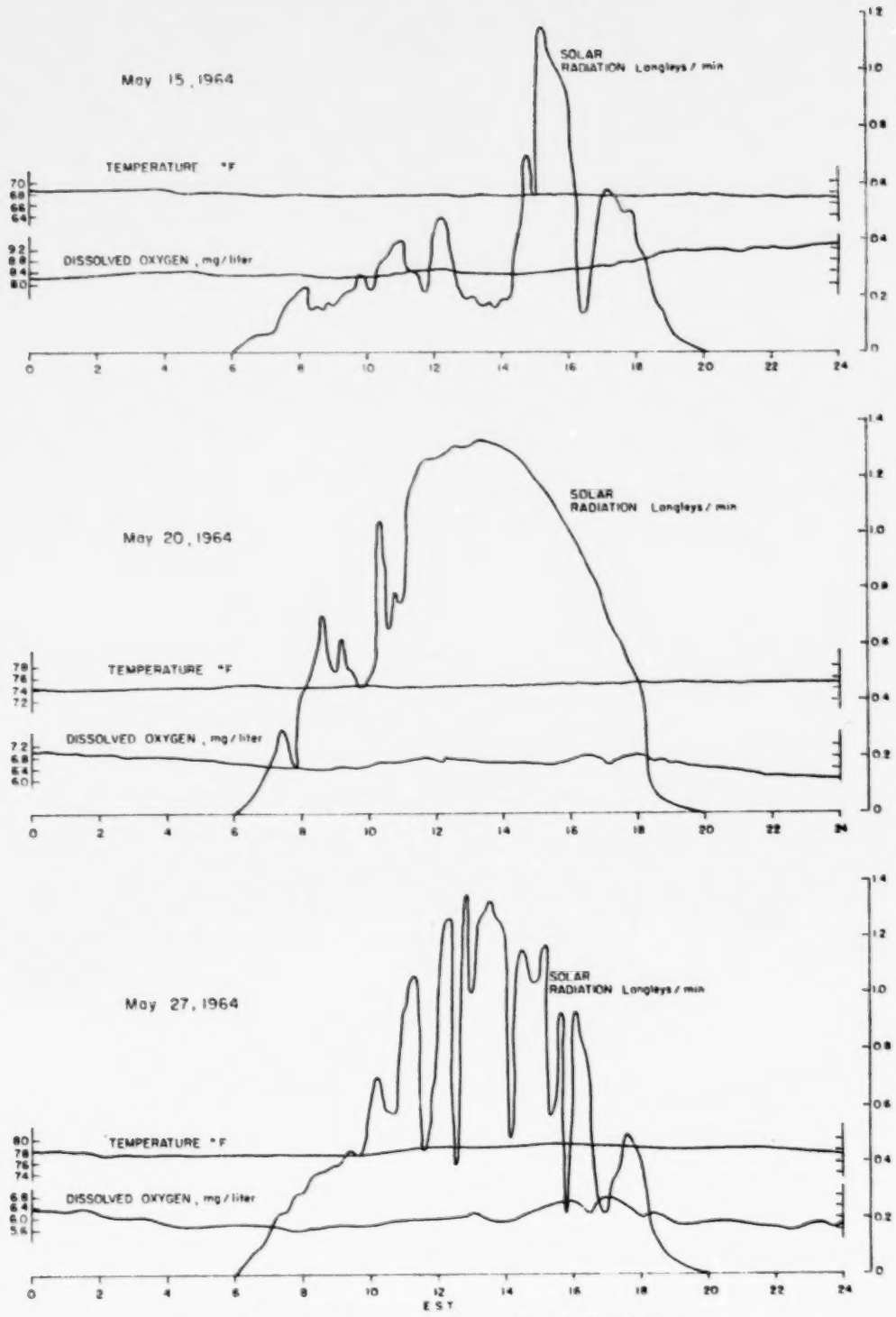

Figure 8A. Comparison of short-term variations in temperature, dissolved oxygen, and solar radiation.

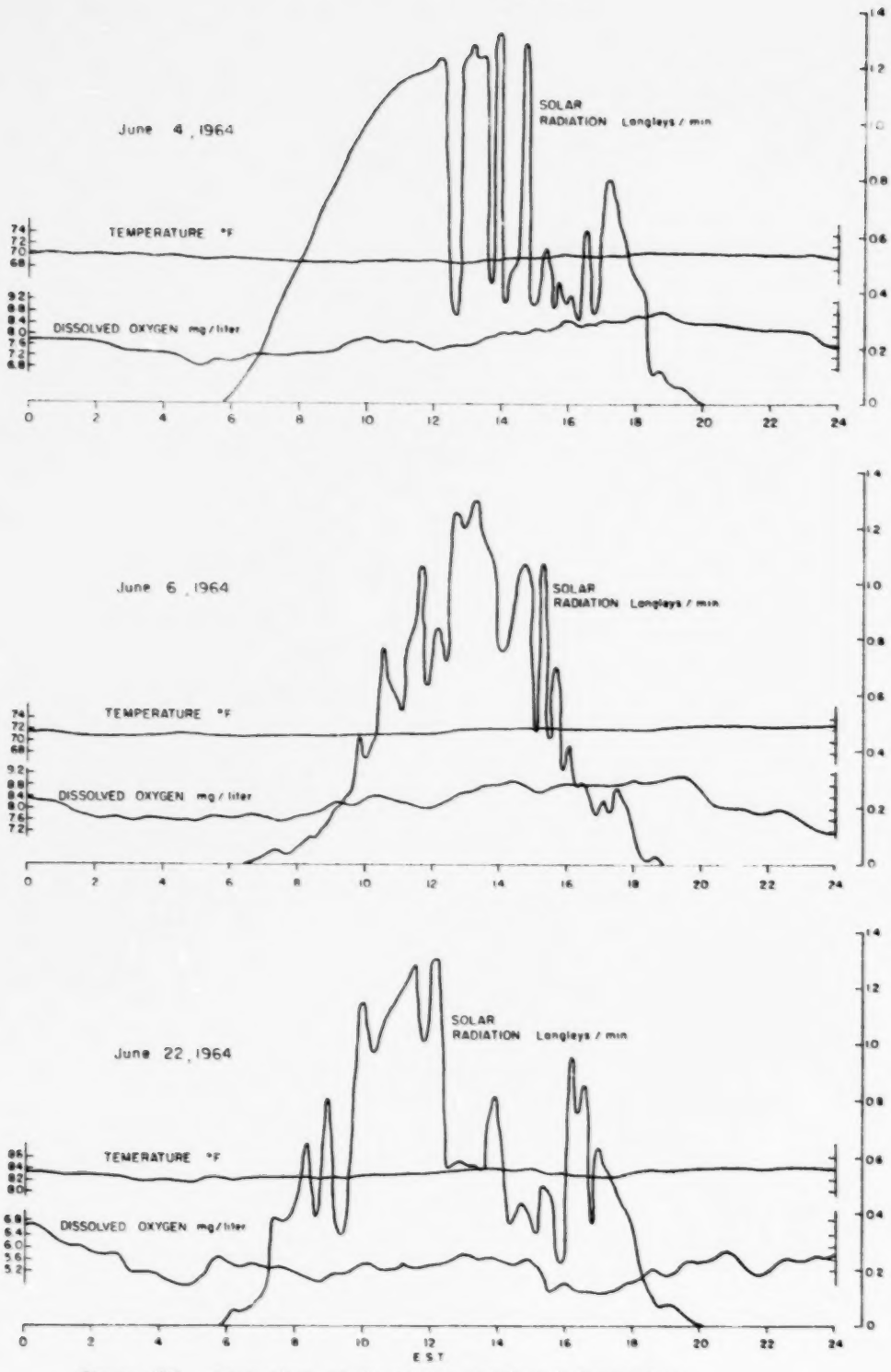

Figure 88. Comparison of short-term variations in temperature, dissolved oxygen, and solar radiation.

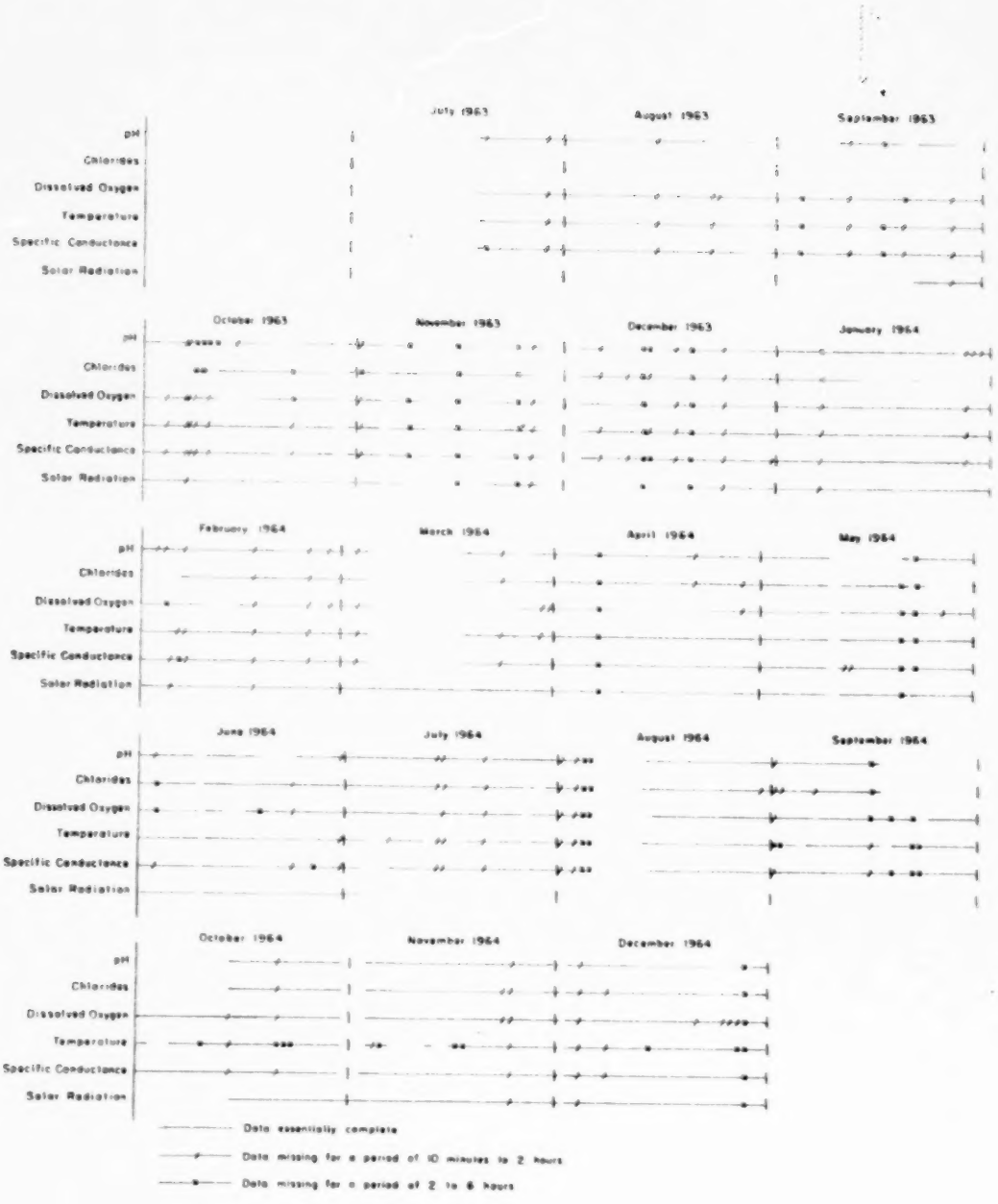

Figure 9. Monitoring equipment operations – July 1963 through December 1964

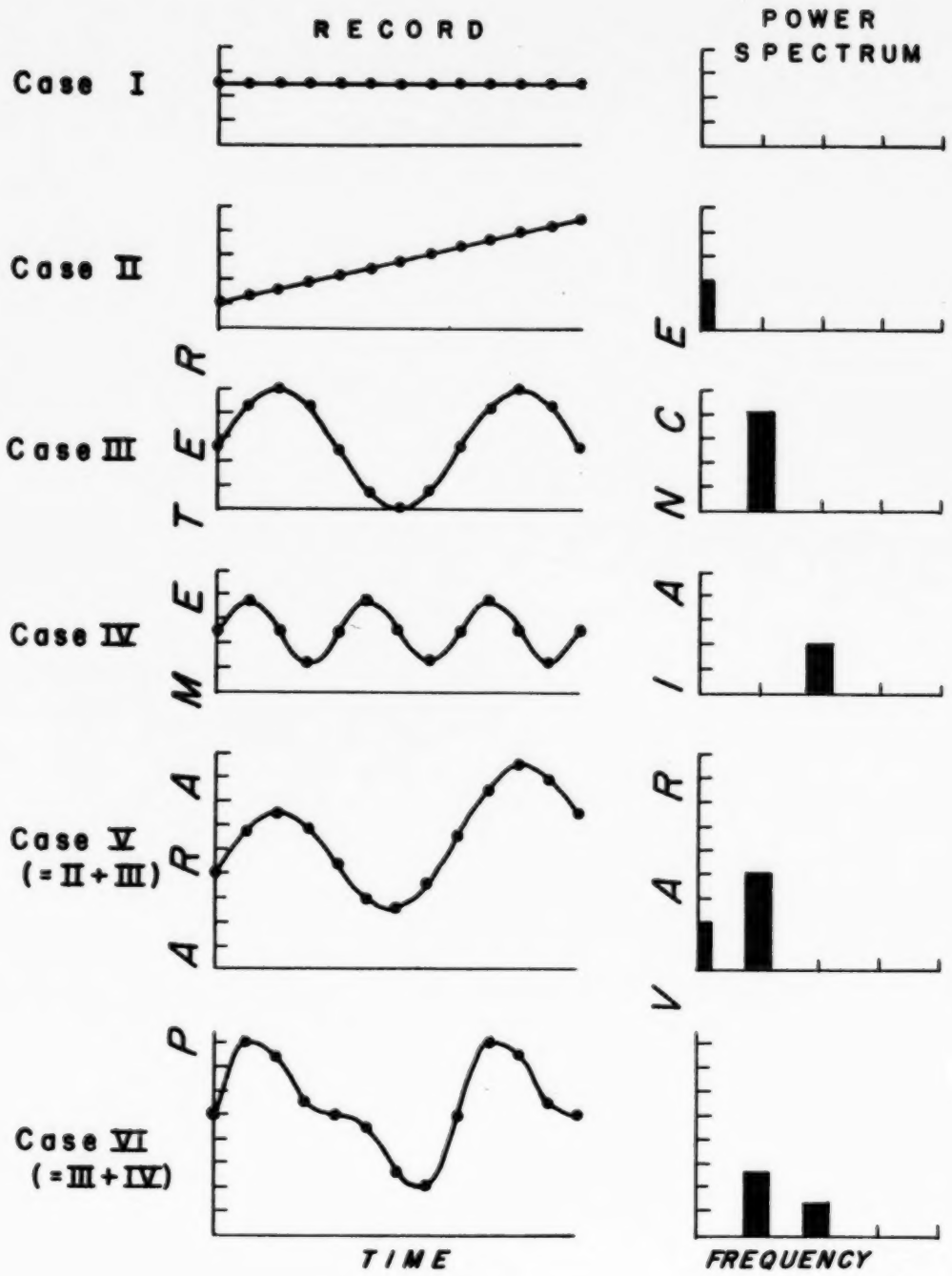

FIGURE AI

SPECTRAL ARITHMETIC

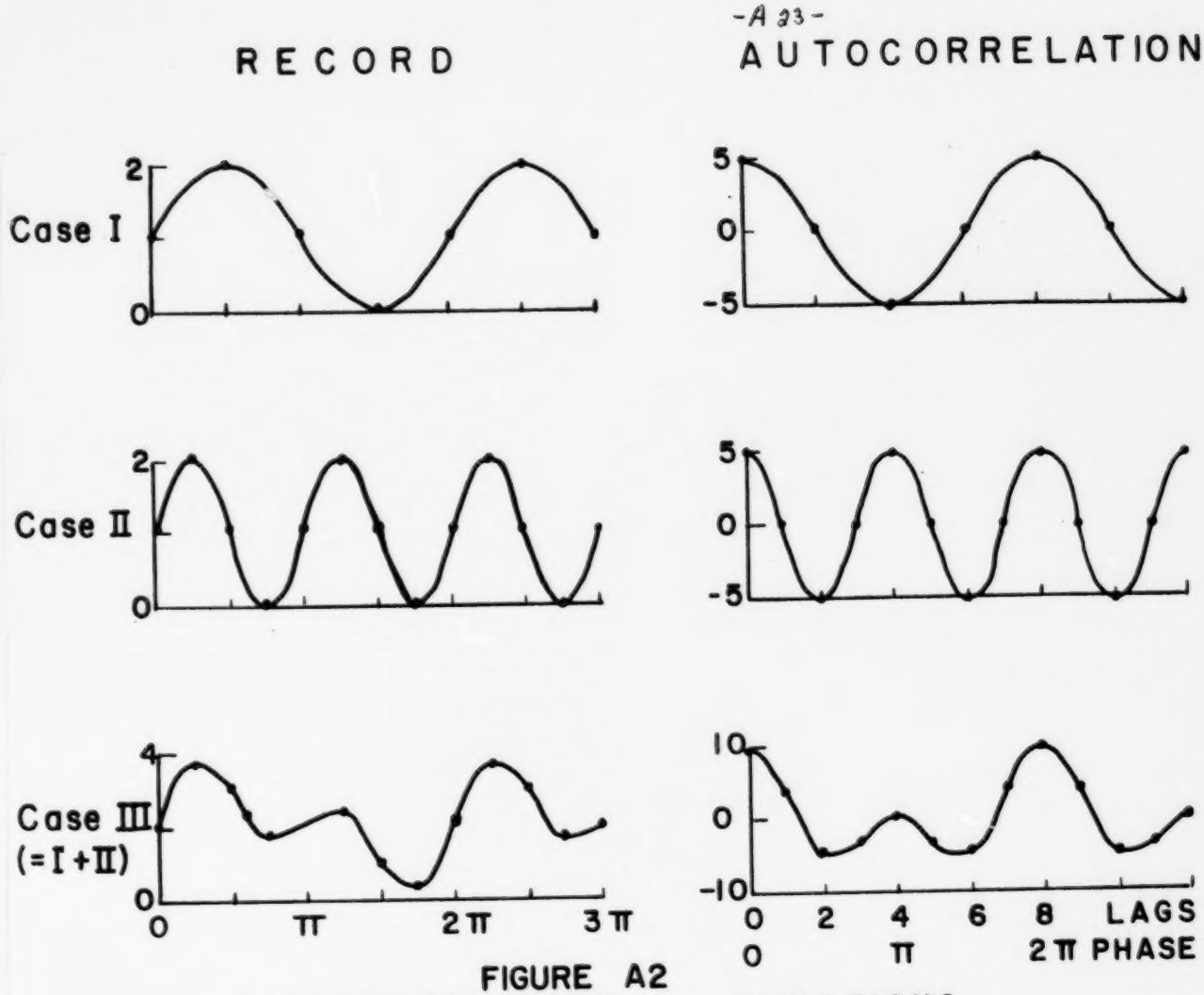

FIGURE A2
AUTOCORRELATION FUNCTIONS
OF SIMPLE SINE WAVES

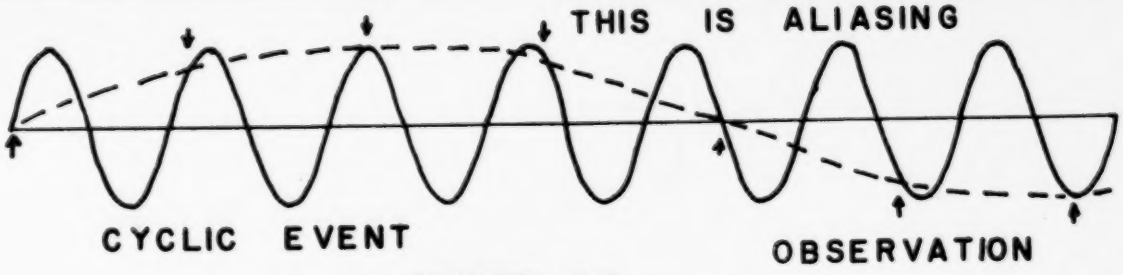

FIGURE A3
RESULT OF OBSERVING OR SAMPLING EVENT AT MORE THAN ONE HALF THE PERIOD OF THE EVENT